Model Based Algebraic Weight Selection for LQI Control Reducing Dog Clutch Engagement Noise

2024-01-2146 Published 09 Apr 2024

Model Based Algebraic Weight Selection for LQI Control Reducing Dog Clutch Engagement Noise

Muddassar Piracha and Anders Grauers Chalmers University of Technology

Johan Hellsing CEVT China Euro Vehicle Technology

Citation: Piracha, M., Grauers, A., and Hellsing, J., "Model Based Algebraic Weight Selection for LQI Control Reducing Dog Clutch Engagement Noise," SAE Technical Paper 2024-01-2146, 2024, doi:10.4271/2024-01-2146.

Received: 23 Oct 2023 Revised: 19 Jan 2024 Accepted: 19 Jan 2024

Abstract

This paper presents a feedback control strategy to minimize noise during dog clutch engagement in a hybrid powertrain. The hybrid transmission contains an internal combustion engine(ICE) and 2 electric motors in P1 and P3 configurations. For efficiency during driving, at high vehicle speeds ICE is connected to wheels, via the dog clutch, hence shifting the vehicle from series to parallel hybrid mode. It is shown by experimental results that if the speed difference between the two sides of the dog clutch is below a certain level the engagement will be without clonk noise. In this paper the designed state feedback Linear Quadratic Integral (LQI) control provides the synchronization torque request to the P1 motor, hence matching the speed of one side of dog clutch with the other under the disturbance from combustion torque of the engine. Normally LQI controllers are tuned by trial-and-error methods, but this paper presents an algebraic approach where the feedback gains of the LQI controller are calculated based solely upon the physical parameters of the system, the required time for speed synchronization and acceptable values of speed difference from experimental results. This approach minimizes the need for manual tuning and can deliver the controller gains for any size and version of the transmission by just modifying the parameter values and functional requirements. The results are shown by simulations on a 2DOF torsional system representing ICE, dual mass flywheel and P1 electric motor.

Introduction

Schematic view of the hybrid powertrain is shown in Figure 1.

The internal combustion engine (ICE) is connected to dual mass flywheel (DMF) which in turn is connected to the P1 electric motor. P1 electric motor is connected to primary side of the dog clutch shown in red in Figure 1 and the secondary side of the dog clutch shown in green is connected to the P3 electric motor, which is then connected to wheels via a gear ratio. Power is supplied to the P3 motor by the battery. Power levels of P3 is 100-150 kW depending on the vehicle size. ICE is of similar power level.

FIGURE 1 Hybrid Powertrain

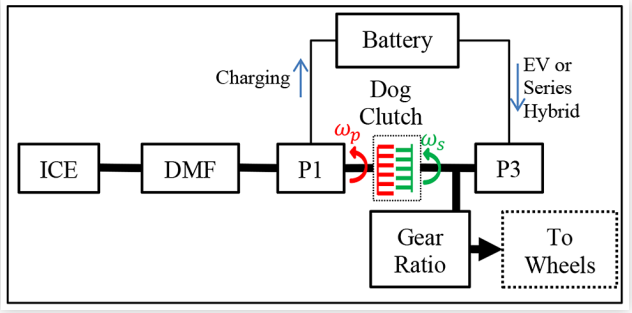

While driving the vehicle can be in the following modes and power flowing to and from the battery in different modes is shown in Figure 1.

1. Pure Electric
2. Series Hybrid
3. Parallel Hybrid

In pure electric mode the engine is shut off, the dog clutch is open and P3 is providing the driving torque to the wheels. The power flow from the battery to P3 motor is shown in Figure 1.

When state of charge in the battery can be low the vehicle is shifted to series hybrid mode. Then the P1 motor can take power from the battery and is used as engine starter motor. Once the engine is running, it is used as a range extender and the battery is charged by P1 motor.

When the vehicle speed is larger than a particular value v_1, for efficiency the vehicle should be in the parallel hybrid mode. In parallel mode the dog clutch is closed, hence connecting the ICE to wheels. Switching the driving

mode from pure electric or series hybrid mode to parallel driving mode consists of 3 distinct phases.

1. Speed synchronization
2. Dog clutch engagement
3. Torque Ramp up

In the first phase "Speed synchronization" the rotational speed of primary side of dog clutch, ω_p, in Figure 1 is controlled, by means of the P1 motor, to match the rotational speed of secondary side of dog clutch ω_s. The speed difference between ω_p and ω_s at the end of phase 1 determines the noise generated in phase 2, "Dog Clutch Engagement". Experimental results presented in this paper show the limits on speed difference at the end of phase 1 which will lead to noise-less dog clutch engagement.

To minimize the speed difference, torque request on P1 motor is calculated by the feedback controller designed in the later sections of the paper. From Figure 1, it can be seen that primary side of dog clutch consists of 2 inertias i.e. ICE and P1 connected by an elastic coupling in the dual mass flywheel. The LQI control of such two degree of freedom (2 DOF) system is designed in [1] and [2]. An algebraic approach for calculating the weighting matrices of an LQ controller based on algebraic Riccati equation is given in [3]. This paper extends the method to LQI controllers, while clearly defining the weighting matrices based on physical parameters of the two-inertia system, the required speed synchronization time and limits on speed difference at the end of speed synchronization. This new approach minimizes the need for manual tuning of the controller, while fulfilling the stability and noise rejection requirements.

Mode Switch from Series Hybrid to Parallel

Figure 2 shows the first two phases of the mode switch during vehicle acceleration.

When the vehicle speed is less than a particular value v_{init}, P1 motor is running in generator mode and is applying a constant braking torque on the engine. When vehicle speed is larger than v_{init} "Speed Synchronization" is started by increasing the braking torque of P1 motor until the right engine speed is reached. This braking torque during speed synchronization is calculated by the feedback controller explained in the later sections of the paper.

Speed synchronization between primary and secondary side can also be achieved by cutting the fuel to the engine and letting the primary side speed decrease under friction. But it is much more controllable to use braking torque from P1 motor torque.

Speed synchronization takes time t_{synch}. It is assumed that ω_s after time t_{synch} is accurately predicted by the electric powertrain on the secondary side of the dog

FIGURE 2 Mode switch wrt time

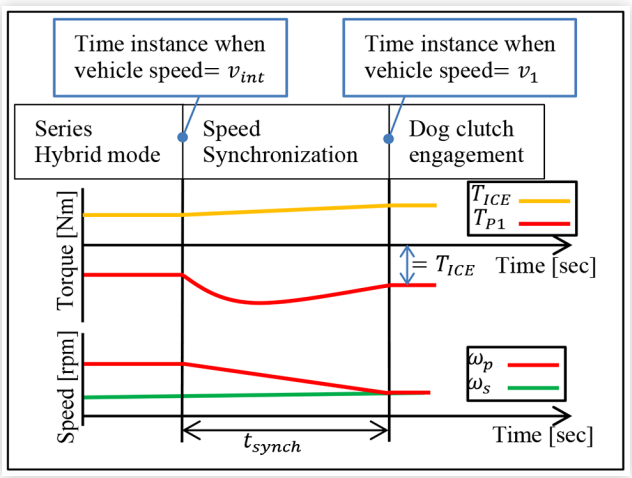

clutch. Based on vehicle acceleration a_{veh}, time t_{synch} and speed v_1, v_{init} can be calculated by

$$v_{init} = v_1 - a_{veh} t_{synch} \tag{1}$$

For this paper

$$t_{synch} = 2\,sec \tag{2}$$

Since speed synchronization is not time critical for this particular transmission, 2 seconds is a reasonable choice. Once the speed synchronization is finished, the second phase "Dog clutch engagement" is started. If the speed is matched perfectly there will be minimum noise and wear in the transmission. The speed difference ω_{diff} is defined as

$$\omega_{diff} = \omega_p - \omega_s \tag{3}$$

To minimize noise and wear ω_{diff} must be within certain limits before the dog clutch is engaged, as discussed in later sections of this paper.

After dog clutch engagement the torque at the wheels will be the sum of the torque from ICE, P1 and P3 motor. To keep a smooth acceleration of the vehicle during the mode shift the torque from all sources needs to be managed such that the toque demand for constant acceleration is fulfilled during the whole mode shift.

From the above section it can be concluded that the first phase in mode switch i.e. speed synchronization is not time critical. Depending on the power available for the P1 electric motor for speed synchronization, synchronization time t_{synch} will change, hence changing the speed v_{init} when the speed synchronization should start. As opposed to transmissions in conventional powertrains, where mode switch and speed synchronization is a time critical problem for fulfilling the torque request, the controller design in this paper will be focused on speed synchronization and dog clutch engagement without noise and wear.

Engagement Test

The actuation mechanism and the dog clutch are shown in Figure 3.

Sleeve and hub are collectively called the primary side of dog clutch and they are shown in Figure 3a. Figure 3b shows the side view of the disengaged dog clutch, as shown the schematic diagram at the top. P1 electric motor is connected to the hub by spline connection as shown in Figure 3a and P3 motor is connected to secondary side by the gear ratio as shown in Figure 3b.

The forces and velocities involved on primary and secondary dog teeth, during the engagement process are shown in Figure 4.

Figure 4a shows the disengaged dog clutch at the end of speed synchronization phase. Primary dog teeth are moving with a rotational speed ω_p and secondary side dog teeth are moving with rotational speed ω_s.

When the shifter motor is rotated in the shift direction shown by the white arrow in Figure 3 the fork will move the sleeve with an axial velocity $\dot{x}_p$ as shown in Figure 4b. The rotational speed difference can be simplified by assuming that the secondary teeth are at rest and the primary teeth are rotating with the speed difference ω_{diff} defined by equation 3

Since the primary side speed ω_p is being controlled by the feedback controller and ω_s is proportional to the vehicle speed, it can be assumed that, for the short time instance of Engaging phase, ω_{diff} will be constant.

When the primary dog teeth have moved a certain distance at time t_{imp}, they will come into contact with the secondary dog teeth as shown in Figure 4c. Depending on the axial speed $\dot{x}_p$ and the rotational speed difference ω_{diff} at t_{imp}, an impact force F_{imp}, normal to the impact surface, will be generated on both teeth. The impact force will increase with the increasing $\omega_{diff}(t_{imp})$ and $\dot{x}_p$ and is responsible for noise and wear.

The axial component F_{xi} of the impact force F_{imp} shown in Figure 4c will resist the engagement and is overcome by the shifter motor shown in Figure 3. Once the primary dog teeth have moved a certain distance and are engaged with the secondary dog teeth, at time t_{end}, the 3rd phase of the mode shift "Torque Ramp up" can be started.

At time t_{imp}, when the dog teeth collide, the tangential component of the impact force F_{yi} will affect the rotational velocities ω_p and ω_s of the dog teeth. The effect can be measured by angular acceleration α_{imp} of the teeth. According to [4] α_{imp} at impact can be defined by

$$\alpha_{imp} = constant\, F_{yi} \tag{4}$$

The maximum value of the acceleration α_{imp} will be at the time instance t_{imp} and is denoted by $[\alpha_{imp}]$

During normal operation of the vehicle, $\omega_{diff}(t_{synch})$ must be very close to zero before the dog clutch engagement. Lab tests were done by engaging the dog clutch at different values of $\omega_{diff}(t_{synch})$ and measuring the maximum instantaneous angular acceleration and the noise from the dog clutch. The results are shown in Figure 5.

FIGURE 3 Mechanical system of Dog clutch

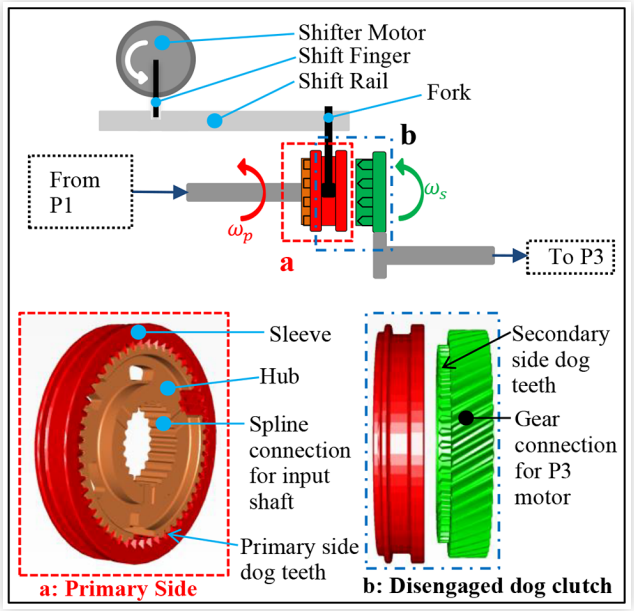

FIGURE 4 Dog teeth during engagement

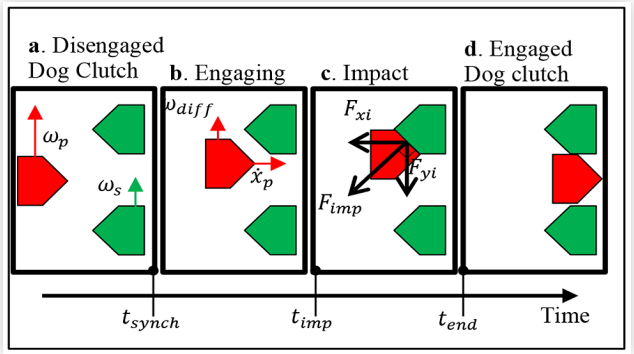

FIGURE 5 Lab Tests

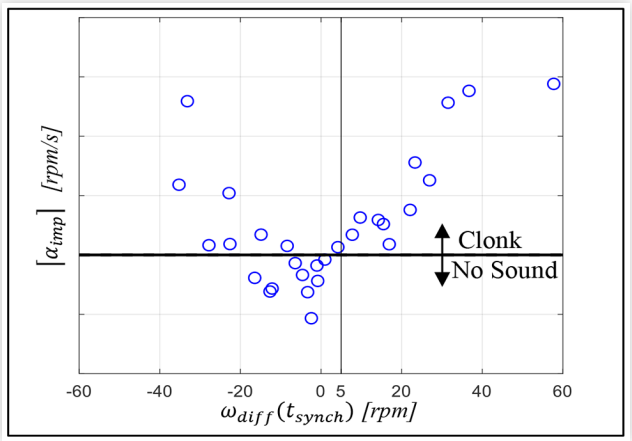

FIGURE 6 Symmetry of F_{imp} vs ω_{diff}

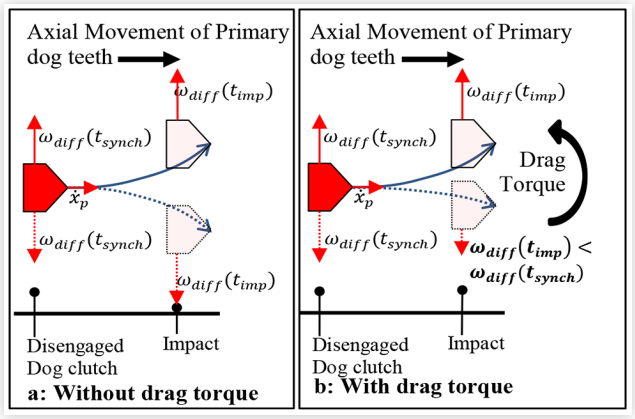

It can be seen from Figure 5, that if α_{imp} is higher than a particular value clonk sound is heard during engagement. As shown in equation 4 a higher α_{imp} means a higher impact force F_{imp}. Higher impact force F_{imp} is in turn a result of a higher ω_{diff}. From Figure 5, it can be seen that if $\omega_{diff}(t_{synch})$ is between –20 *and* 5 *rpm* there will most probably be no clonk sound.

During the lab tests shown in Figure 5, the primary side speed ω_p is not controlled, so from time instance t_{synch} to t_{end} the rotational speed difference ω_{diff} is not constant due to drag torque in the transmission.

Ideally, the pattern of points in Figure 5, should be centered around zero ω_{diff}, as α_{imp} is a function of absolute value of ω_{diff}. As shown in Figure 6a, if there is no drag torque in the transmission, then $\omega_{diff}(t_{synch})$ will be equal to $\omega_{diff}(t_{imp})$, so the impact force would be the same irrespective of the direction of ω_{diff}. Drag torque on either primary or secondary side can be represented by the directional drag torque shown in Figure 6b.

The effect of directional drag torque will be different depending on the direction of ω_{diff}. For the drag torque shown in Figure 6b, it can be seen that $\omega_{diff}(t_{imp})$ is less than $\omega_{diff}(t_{synch})$, if ω_{diff} is in downwards direction resulting in lower F_{imp} and α_{imp} than if ω_{diff} is in upwards direction. Consequently the noise produced by the impact will be lower if ω_{diff} is in downwards direction. The same kind of test results are reported for a flat teeth dog clutch by [5].

For this paper based on Figure 5 and Figure 6, it can be safely assumed that

$$\left|\omega_{diff}\left(t_{synch}\right)\right| < 5rpm \underset{results}{\Rightarrow} No\,Clonk \tag{5}$$

Controller Design

To control the primary speed ω_p to right value before the dog clutch can be engaged, toque control of the P1 electric machine is used. However, due to the dual mass flywheel and the time variations of the engine torque, this is not trivial. To ensure a fast, accurate and robust control of the primary speed a controller is designed in the following section.

Model of Primary Side of the Transmission

The components on the primary side of the dog clutch can be represented by a 2 DOF torsional system are shown in Figure 7.

The torque from the engine acts on one side of the system, and the P1 motor torque on the other side. In between are several inertias, which can be lumped together into two inertias connected via a torsional spring and damper. The two inertias are

$$\begin{aligned} J_p &= J_{Hub\&Sleeve} + J_{P1\ rotor} + J_{DMF\ secondary} \\ J_e &= J_{crankshaft} + J_{Flywheel} + J_{DME\ primary} \end{aligned} \tag{6}$$

The torque T_{DMF} applied by the torsional spring and damper of the DMF on both the inertias J_p and J_e is

$$T_{DMF} = d\left(\omega_p - \omega_e\right) + k\left(\theta_p - \theta_e\right) \tag{7}$$

Defining $\Delta\theta$, such that

$$\Delta\theta = \theta_p - \theta_e \tag{8}$$

Applying Newton's 2nd law on inertia J_p and J_e a set of two differential equations describing the speed dynamics of the system are obtained

$$\begin{aligned} J_p\dot{\omega}_p &= -d\omega_p - k\Delta\theta + d\omega_e + T_{P1} \\ J_e\dot{\omega}_e &= -d\omega_p + k\Delta\theta - d\omega_e + T_{ICE} \end{aligned} \tag{9}$$

Differentiating equation 8 on both sides

$$\Delta\dot{\theta} = \omega_p - \omega_e \tag{10}$$

Combining the differential equations in equations 9 and 10 the linear time invariant state space model of the

FIGURE 7 2DOF torsional system for primary side

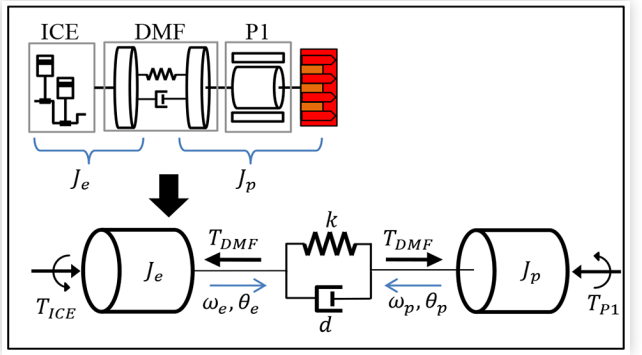

mechanical system in Figure 7 can be obtained by setting the disturbance $T_{ICE} = 0$, such that

$$\begin{aligned} \dot{x} &= Ax + Bu \\ y &= Cx \end{aligned} \tag{11}$$

where state vector x is

$$x = \begin{bmatrix} \omega_p & \Delta\theta & \omega_e \end{bmatrix}^T \tag{12}$$

and

$$A = \begin{bmatrix} -d/J_p & -k/J_p & d/J_p \\ 1 & 0 & -1 \\ d/J_e & k/J_e & -d/J_e \end{bmatrix} = \begin{bmatrix} -a_1 & -a_3 & a_1 \\ 1 & 0 & -1 \\ a_2 & a_4 & -a_2 \end{bmatrix} \tag{13}$$

$$B = \begin{bmatrix} 1/J_p & 0 & 0 \end{bmatrix}^T = \begin{bmatrix} b & 0 & 0 \end{bmatrix}^T \tag{14}$$

The constants a_1 to a_4 in equation 13 and constant b in equation 14 are positive numbers and depend on the physical constants of the system.

Vector C in equation 11 will be

$$C = \begin{bmatrix} 1 & 0 & 0 \end{bmatrix} \tag{15}$$

since only the first state ω_p i.e. the primary side dog teeth speed is to be controlled during speed synchronization.

Feedback Controller

For synchronizing the speed of the primary side of the dog clutch the input u to the system will be the torque request from P1 motor so

$$u = T_{P1} \tag{16}$$

A linear state feedback controller is chosen because it can be easily implemented in the existing transmission control software. In Figure 8 the plant model is shown in blue, and a state feedback controller in black, where K is the linear state feedback gain.

FIGURE 8 Linear State feedback control system

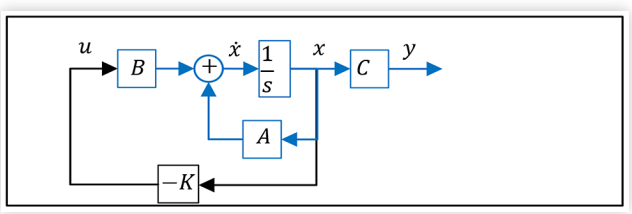

FIGURE 9 Definition of reference $\omega_{p\,ref}$

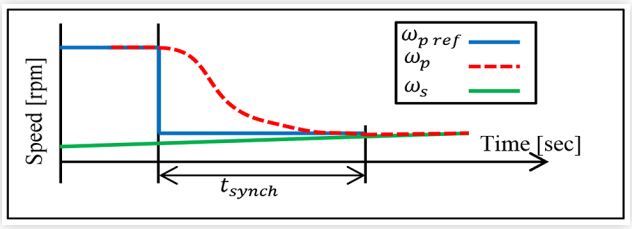

From Figure 8 the torque request on P1 motor in equation 16 can be rewritten as

$$u = -Kx \tag{17}$$

In order to minimize the speed difference ω_{diff} in equation 3 under the disturbance from T_{ICE}, the first state of the system in equation 12 ω_p, needs to reach the target speed shown by $\omega_{p\,ref}$ as shown in Figure 9.

From Figure 9, it can be seen that at time t_{synch}, $\omega_{p\,ref}$ is equal to ω_s, so if ω_p reaches $\omega_{p\,ref}$, after time t_{synch}, dog clutch can be engaged without noise. To analyze the control of the speed an error ε can be introduced

$$\varepsilon = \omega_{p\,ref} - \omega_p \tag{18}$$

Adding the integral of the error ε in the system (11) as an additional state, an integral action of the feedback control is obtained which will eliminate the steady state error. With this new state the augmented state space model will be

$$\begin{aligned} \begin{bmatrix} \dot{x} \\ \varepsilon \end{bmatrix} &= A_{aug}x + B_{aug}u + \begin{bmatrix} 0 \\ 1 \end{bmatrix} \omega_{p\,ref} \\ y &= C_{aug} \begin{bmatrix} x \\ \varepsilon \end{bmatrix} \end{aligned} \tag{19}$$

where

$$A_{aug} = \begin{bmatrix} A & 0 \\ -C & 0 \end{bmatrix}, B_{aug} = \begin{bmatrix} B^T & 0 \end{bmatrix}^T, C_{aug} = \begin{bmatrix} C & 0 \end{bmatrix} \tag{20}$$

The feedback control system in Figure 8 updated with the integral state and reference $\omega_{p\,ref}$ is shown in Figure 10.

FIGURE 10 Reference tracking integral control system

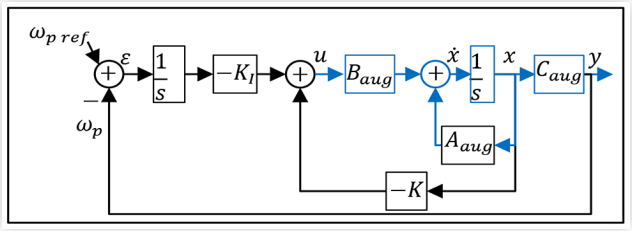

From Figure 10 the torque request on P1 motor u can be rewritten as

$$u = -Kx - K_I \int_0^t \varepsilon.dt \tag{21}$$

LQI Control

The state feedback can be selected in many ways, but generally it is required to find a controller gain that is optimal regarding some criteria. One way to find an optimal feedback control law for equation 21 can be obtained by solving infinite time linear quadratic problem, which results in a LQI control. This type of controller outputs the control input u that minimizes the criteria J where

$$J = \int_0^\infty [x^T \epsilon] Q [x^T \epsilon]^T + u^T r u \tag{22}$$

By using this method the resulting controller will be robust and inherently stable [3].

Matrix Q and scalar r in equation 22 can be defined as

$$Q = \begin{bmatrix} q_1 & 0 & 0 & 0 \\ 0 & q_2 & 0 & 0 \\ 0 & 0 & q_3 & 0 \\ 0 & 0 & 0 & q_4 \end{bmatrix} and\, r > 0 \tag{23}$$

The elements of matrix Q and r, define the weights on states and control input in the criteria to be minimized (22). When determining the LQI controller gain, the absolute values of Q and r, are not important. Rather, it is their relative values which determines the feedback gain of the controller. A relative high value on q_4 for instance means that keeping the integral error ε small, is more important than keeping the other states or the control effort small. A very high value on r means that it is more important to keep the control effort u small, than to keep the state errors small.

The feedback gains K and K_I in equation 21 can, for an LQI controller, be calculated by

$$\begin{bmatrix} K & K_I \end{bmatrix} = r^{-1} B_{aug}^T P \tag{24}$$

where P is the solution to the Algebraic Riccati equation i.e.

$$PA_{aug} + A_{aug}^T P - PB_{aug} r^{-1} B_{aug}^T P + Q = 0 \tag{25}$$

and is a symmetric matrix of the form

$$P = \begin{bmatrix} p_{11} & p_{12} & p_{13} & p_{14} \\ p_{12} & p_{22} & p_{23} & p_{24} \\ p_{13} & p_{23} & p_{33} & p_{34} \\ p_{14} & p_{24} & p_{34} & p_{44} \end{bmatrix} \tag{26}$$

Controller Synthesis

Previous research has shown some methods to find the values of Q and r in equation 22. They are experimentally found in [1] and [2] without using the Q in the diagonal form shown in equation 23 . In [3] the diagonal form of Q is used, and Q and r are calculated based on characteristic equations of the closed loop system. But the characteristic equation is based on the *controllable canonical form* of the system instead of *the augmented system* shown in equation 19. To keep the values of feedback gains in equation 24 dependent on the physical parameters of the system, in this paper controllable canonical form will not be used.

The core idea of the method for controller calibration in the following sections of this paper is to

- Minimize the need for manual tuning
- Be based on physical properties of the system and functional requirements so it can be used on any size and version of the transmission without needing to change anything other than parameter values
- Guaranteed stability
- Low steady state error
- Noise rejection

The characteristic equation of the closed loop system in Figure 10 can be written as

$$det(sI - A_{aug} + B_{aug}[K\ K_I]) = 0 \tag{27}$$

where I is the identity matrix and s is the Laplace variable

Substituting K from equation 24 in equation 27

$$\det\left(sI - A_{aug} + B_{aug} r^{-1} B_{aug}^T P\right) = 0 \tag{28}$$

Roots of equation 28 define the poles of the closed loop system and hence define time response of the system. The system in equation 19 is a fourth order system, so 4 poles need to be decided. Once the poles of the system are decided, the solution P to algebraic Riccati equation can be calculated and then feedback gains in equation 24 will be calculated.

Choosing Poles of the Closed Loop System

The transfer function of a 4th order system is

$$G(s) = \frac{w_n^2}{s^4 + 4\xi w_n s^3 + w_n^2\left(2 + 4\xi^2\right)s^2 + 4\xi w_n^3 s + w_n^4} \tag{29}$$

where w_n is the natural frequency and ξ is the damping ratio.

Figure 11 shows the response of a fourth order system with fixed natural frequency w_n and variable damping ratios ξ.

FIGURE 11 Response of a fourth order system

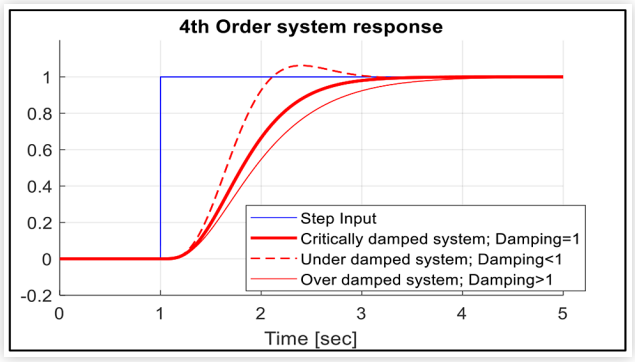

In Figure 11, it can be seen that the critically damped response reaches the steady state value in the least time. The under damped response is faster to reach the desired speed but does not stay there and continues and produces an overshoot. Since in this paper the control problem deals with speed synchronization, an overshoot will create NVH issues so, a critically damped system is chosen.

With $\xi = 1$, and *input*(s) being a unit step the transfer function in equation 29 becomes

$$output(s) = \frac{1}{s}\frac{w_n^2}{s^4 + 4w_n s^3 + 6w_n^2 s^2 + 4w_n^3 s + w_n^4} \quad (30)$$

Using partial fractions equation 30 becomes

$$output(s) = \frac{1}{s} - \frac{1}{s+w_n} - \frac{w_n}{(s+w_n)^2} - \frac{w_n^2}{(s+w_n)^3} - \frac{w_n^3}{(s+w_n)^4} \quad (31)$$

Taking Laplace inverse on both sides of equation 31

$$output(t) = 1 - e^{-w_n t}\left(1 + w_n t + \frac{w_n^2 t^2}{2} + \frac{w_n^3 t^3}{3}\right) \quad (32)$$

Equation 32 can be solved by using Figure 12 which shows the step response of a critically damped fourth order system.

In Figure 12 if step input is $\omega_{p\,ref}$ from Figure 9, the output will be ω_p. The error ε in equation 18 can be used with equation 5 to define error $\varepsilon(t_{synch})$. If $\varepsilon(t_{synch})$ is within the limits defined in equation 5, the dog clutch can be engaged without noise after time t_{synch}.

Equation 32, represents the evolution of *output* or ω_p with time. The requirement on ω_p is such that after time t_{synch} it should reach $\omega_s(t_{synch})$ within error bounds defined by equation 5. So equation 32 can be rewritten as

$$\frac{limits\ of\ \omega_{diff}}{\omega_s(t_{synch})} = e^{-w_n t_{synch}}\left(1 + w_n t_{synch} + \frac{w_n^2 t_{synch}^2}{2} + \frac{w_n^3 t_{synch}^3}{3}\right) \quad (33)$$

FIGURE 12 Step response of a critically damped 4th order system

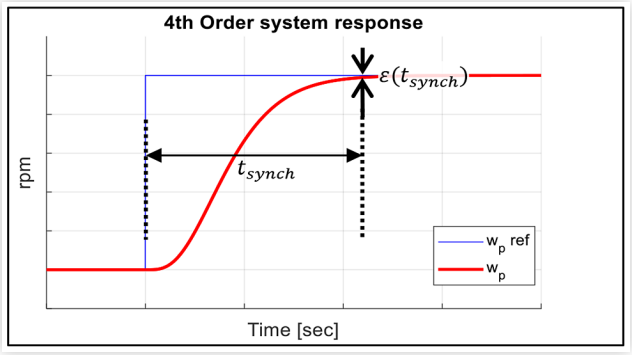

Since equation 33 has one unknown w_n it can be solved, and the solution will be of the form

$$w_n = constant / t_{synch} \quad (34)$$

Equation 34 represents the location of four poles of the transfer function in equation 29.

Calculating Solution to Riccati Equation and Feedback Gain

In this step value of w_n from equation 34 will be used in denominator polynomial of transfer function in 29 to determine the elements in the *P* matrix.

By comparing the coefficients for s^3, s^2, s and the constant term in equation 28 with denominator polynomial of 29 following equation set is obtained, the unknowns are shown in red

$$\begin{aligned}
&a_1 + a_2 + p_{11} * \frac{b^2}{r} = 4\xi w_n \\
&\frac{b^2}{r} * p_{12} - \frac{b^2}{r} * p_{14} + a_2 * \frac{b^2}{r} * p_{11} \\
&+a_2 * \frac{b^2}{r} * p_{13} + a_3 + a_4 = w_n^2\left(2 + 4\xi^2\right) \\
&a_4 * \frac{b^2}{r} * p_{11} - a_2 * \frac{b^2}{r} * p_{14} + a_4 * \frac{b^2}{r} * p_{13} = 4\xi w_n^3 \\
&-a_4 * \frac{b^2}{r} * p_{14} = w_n^4
\end{aligned} \quad (35)$$

The equation set 35 has four unknowns p_{11}, p_{12}, p_{13} *and* p_{14} and four equations so a unique solution can be calculated by setting *r* an arbitrary positive number.

After solving equation set 35, there will be 6 remaining unknown elements left in the *P* matrix in equation 26, also the 4 elements of *Q* matrix in equation 23 need to be calculated. This requires 10 equations that can

be obtained from matrix equation 25, the unknowns are shown in red

$$
\begin{aligned}
&2p_{12} - 2p_{14} + q_1 - 2a_1p_{11} + 2a_2p_{13} - \frac{b^2p_{11}^2}{r} = 0\\
&p_{22} - p_{24} - a_1p_{12} - a_3p_{11} + a_4p_{13} + a_2p_{23} - \frac{b^2p_{11}p_{12}}{r} = 0\\
&p_{23} - p_{12} - p_{34} + a_1p_{11} - a_1p_{13} - a_2p_{13} + a_2p_{33} - \frac{b^2p_{11} * p_{13}}{r} = 0\\
&p_{24} - p_{44} - a_1p_{14} + a_2p_{34} - \frac{b^2p_{11}p_{14}}{r} = 0\\
&q_2 - 2a_3p_{12} + 2a_4p_{23} - \frac{b^2p_{12}^2}{r} = 0\\
&a_1p_{12} - p_{22} - a_3p_{13} - a_2p_{23} + a_4p_{33} - \frac{b^2p_{12}p_{13}}{r} = 0\\
&a_4p_{34} - a_3p_{14} - \frac{b^2p_{12}p_{14}}{r} = 0\\
&q_3 - 2p_{23} + 2a_1p_{13} - 2a_2p_{33} - \frac{b^2p_{13}^2}{r} = 0\\
&a_1p_{14} - p_{24} - a_2p_{34} - \frac{b^2p_{13}p_{14}}{r} = 0\\
&q_4 - \frac{b^2p_{14}^2}{r} = 0
\end{aligned}
\tag{36}
$$

After solving equation set 36, the six remaining elements of P matrix that were p_{22}, p_{23}, p_{24}, p_{33}, p_{34} and p_{44} will be calculated along with the 4 elements of matrix Q, which are q_1, q_2, q_3 and q_4.

Once solution P to the Riccati equation in equation 26 is calculated the linear feedback gains K and K_I can be calculated by equation 24, hence concluding the controller design.

Summary

To summarize the control design process feedback gains K and K_I depend on determining the P matrix based on an arbitrarily chosen positive r as shown in equation 24.

Since P is a symmetric matrix as shown in equation 26, it has 10 unknowns instead of 16 unknowns for a non-symmetric matrix. The first row/column of P can be calculated by comparing the characteristic polynomial of the closed loop system in 28 with denominator of a fourth order transfer function in 35.

The denominator can be solved by solving equation 32 for a chosen point in Figure 12.

The rest of the elements in P and diagonal matrix Q can then be solved using Riccati equation.

It is worth noting that the controller design process described in this paper will also work if matrix Q is not in diagonal form as shown in equation 22. If for instance Q matrix is in a form similar to the one shown by [1] or [2] the equation set 36 will be updated accordingly and the system will still have a unique solution if the number of elements in matrix Q are 4.

The resulting controller will be stable since it's a LQI feedback controller, the integral action guarantees low steady state error. Since the poles are chosen for a critically damped system, the response will reach desired value in short time without overshoot.

Defining the Relative Weighting

Substituting value of p_{14} in the last equation of equation set 36 from last equation of equation set 35 following equation is obtained

$$\frac{q_4}{r} = \frac{w_n^8}{a_4^2b^2} \tag{37}$$

Equation 37 shows the relative value between the randomly selected positive weight r on input u and the weight q_4 on the integral error as defined by equation 22 and 23. It can be seen from equation 37 that the relative value depends on a_4 and b, which are physical parameters of the system as defined by equations 13 and 14 and w_n which depends on the desired performance of the system and is derived by functional requirements as shown in equation 33.

Hence, to fulfill the functional requirements for a particular physical system the relative weighting between q_4 and r must be as defined by equation 37. This formulation of relative weighting can be compared to [6], where the relative weight between q_4 and r is determined by trial-and-error method in offline simulations.

It can also be shown that the other weights q_1, q_2 and q_3 relative to, will also solely depend on physical parameters in matrices A and B from equations 13 and 14 and functional requirements defined using Figure 12.

So, the LQI control implementation approach described in this paper gives controller formulation in terms of physical parameters and functional requirements, hence eliminating the need for large number of controller simulation to tune the controller for desired responses. This will save a lot of transmission calibration work, and also eliminate the risk for errors in the calibration process.

Simulation Results

To demonstrate the performance of a controller designed with the presented method Figure 13 shows the angular velocities ω_p and ω_e during speed synchronization.

From Figure 2, when the vehicle speed is lower than v_{init} the ICE and primary side of dog clutch are running at 2000 rpm. At 0.5 seconds in Figure 13, when the vehicle speed becomes larger than v_{init} the speed synchronization starts and primary side speed drops to 1500 rpm within 2 seconds, which is time t_{synch} as defined by equation 2.

Figure 14 shows the control of primary side speed ω_p with the target speed ω_{ref}.

The zoomed in view shown by the green dotted box in Figure 14 shows that ε after time t_{synch} is less than

FIGURE 13 Rotational speed states during speed synchronization

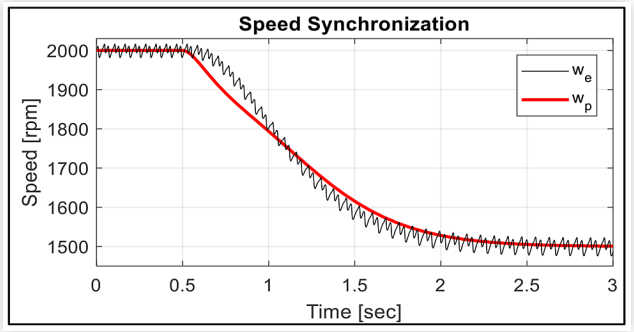

FIGURE 14 Controller performance fulfilling functional requirements

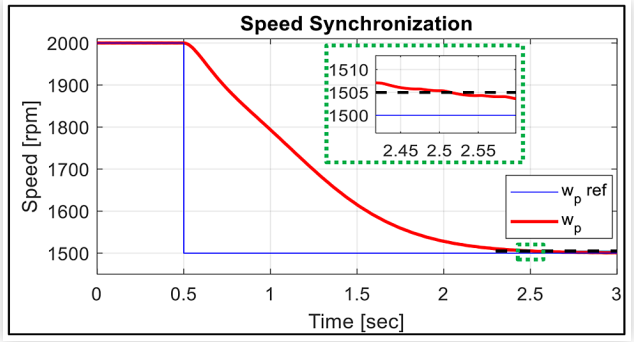

5 rpm so according to equation 5 the following dog clutch engagement will be without clonk noise.

If the functional requirement of t_{synch} is changed from 2 sec from equation 2 to 1 sec, and the controller is redesigned, the new controller's performance is shown in Figure 15 which shows that the synchronization time requirement of 1 sec is fulfilled but the error after time t_{synch} is not within the limits defined by equation 5.

The reason can be seen by investigating the resulting magnitude of q_2 in equation 23, which from equations 22 and 12 is the weight defined for the state $\Delta\theta$ of the system. A high value of q_2 implies that $\Delta\theta$ should be very small. A very small $\Delta\theta$ according to equation 8 means

FIGURE 15 Controller performance for different functional requirements

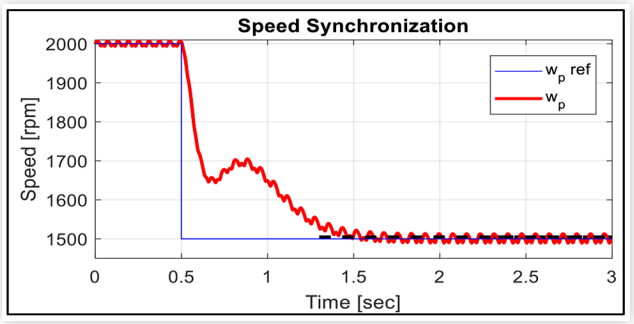

FIGURE 16 Vibration isolation for controllers with different functional requirements with thick dotted lines for t_{synch} = 2 sec and thin dashed lines for t_{synch} = 1 sec

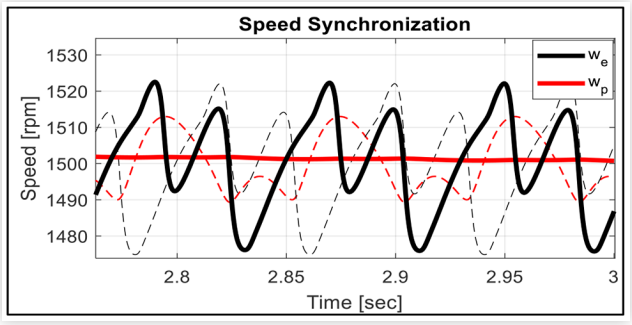

that the vibration isolation between engine and the primary side of dog clutch will be poor. This can be seen by comparing the magnitudes of fluctuations in ω_p for controller designed for t_{synch} equal to1 sec shown by thin dotted red line in and ω_p for t_{synch} equal to 2 seconds shown by thick red line in Figure 16.

From Figure 16, it can be seen that fluctuations in ω_e under the influence of the disturbance T_{ICE} is same for both controllers.

For the controller designed using the approach described the value of q_2 for t_{synch} = 1 sec is 170 times more than that for t_{synch} = 2sec and hence the poor vibration isolation and unfulfillment of error after time t_{synch} in Figure 15 as compared to Figure 14.

For the particular problem of speed synchronization in the hybrid powertrain described in this paper, it is not an issue that the synchronization time is long because the speed synchronization is not time critical. So by decreasing v_{init} in Figure 2, the t_{synch} can be increased according to equation 1 to a level where the noise requirement is fulfilled e.g. t_{synch} being equal to 2sec.

Alternatively a non-diagonal form of Q in equation 23 can be calculated by the iterative method proposed in [6] using desired close loop poles. The desired closed loop poles can be obtained from the method explained in the section "Choosing poles of the closed loop system".

Conclusions

This paper has presented a hybrid transmission in which the combustion engine is connected to wheels at high vehicle speeds. During the mode switch from series to parallel a dog clutch is used. In order to minimize the noise in the dog clutch, during engagement, the dog clutch needs to be synchronized properly. The criterion under which the noise will be minimized in the dog clutch engagement have been shown by experimental results.

A controller design approach is presented for the speed synchronization. The detailed calculation method presented in this paper delivers a feedback LQI controller, whose parameters are solely based upon physical parameters of the transmission and its functional requirements.

This design approach delivers a controller without the need of trial-and-error tuning method usually required for such controllers. The noise rejection and fulfillment of functional requirements of the controller is shown by simulation results run on detailed simulation model of the relevant parts of the transmission.

References

1. Janiszewski, D., "Real-Time Control of Drive with Elestic Coupling Based on Motor Position Only," *IEEE International Symposium on Industrial Electronics*, 2011.
2. Ji, J.-K., and Sul, S. K., "Kalman Filter and LQ Based Speed Controller for Torsional Vibration Suppression in a 2-Mass Motor Drive System," *IEEE Transactions on Industrial Electronics*, 1995.
3. Vinodh, K.E. and Subramanian, R.G., "A New Algebraic LQR Weight Selection Algorithm for Tracking Control of 2 DoF Torsion System," *Archives of Electrical Engineering* (2017): 55-75.
4. Sun, S., Gong, M., Wu, B., and Zou, Y., "Research on Optimal Meshing Speed Difference Based on Shift Success Probability for Dog Clutch in Automated Manual Transmission," *IOP Conference Series: Materials Science and Engineering*, Hangzhou, China, 2020.
5. Achtenova, G., Pakosta, J., and Morsy, M. E., "Smoothness of Maybach Dog Clutch Shift in the Automotive Gearbox," *13th International CTI Symposium*, Berlin, December 2014.
6. Carrière, S., Caux, S., and Fadel, M., "Optimal LQI Synthesis for Speed Control of Synchronous Actuator under Load Inertia Variations," *IFAC Proceedings* 41, no. 2 (2008): 5831-5836.

Contact Information

Muddassar Zahid Piracha
muddassar.piracha@cevt.se
+46 721 84 39 70

ISSN 0148-7191